

Automated Primary Brain Tumors Classification of MR Images using Texture Features Extraction and Machine Learning

Hare Krishna Mishra¹, Dr. Govind Kumar Jha², Krishnanand Mishra³

Submitted:05/07/2023

Revised:07/08/2024

Accepted:17/08/2024

Abstract: Among all cancers, brain cancer has the greatest fatality rates due to its difficult detection and misdiagnosis. The ability to distinguish on the basis of variations in texture, shape, intensity, and deep features, makes Magnetic Resonance Imaging (MRI) a popular tool for the diagnosis of brain cancer. These features have been utilized during the classification of brain tumors. This paper proposes a methodology for classifying primary brain tumors in binary class using the texture features of Magnetic Resonance (MR) images. The Gabor 2D filter, Haralick Texture Features (HTF), Edge Continuity Texture Features (ECTF), First-Order Statistical Texture Features (FOSTF), Local Binary Pattern Texture Features (LBPTF), Difference Theoretic Texture Features (DTTF), and Spectral Texture Features (STF) are used for texture feature extraction of brain MR images. The Tanh normalization method further normalized the retrieved features to deal with outliers and dominant features. The Infinite Latent Feature Selection (ILFS) approach is used for feature ranking to find the most pertinent and non-redundant texture features once the features have been normalized. The top 200-ranked features are used for the classification. The proposed method is compared with different supervised classifiers and achieves high classification accuracy with a minimum error rate and better precision, sensitivity, specificity, Mathew Correction Coefficient (MCC), and F1-Score values. An accuracy of 99.4% has been achieved with the cubic Support Vector Machine (SVM) classifier for the Figshare dataset. A comparison has also been made between the proposed method and other state-of-the-art methods.

Keywords: Brain Tumor, Magnetic Resonance Imaging, Texture Features, Normalization, Classification.

1. Introduction

According to the World Health Organization, brain tumors are mainly classified as primary or secondary brain tumors based on their origin [1]. Primary brain tumors start to develop within the brain cells or the immediate surroundings of the brain [2]; on the other hand, secondary brain tumors develop in the brain due to other body organs, such as the liver, lungs, and kidneys. Most of the brain tumors are primary [3] and are further divided into meningioma, craniopharyngioma, schwannoma, retinoblastoma, astrocytoma, ependymoma, glioma, and pituitary, depending on location in the brain [4]. After getting the location of the brain tumor, it needs to check the aggressiveness of the tumor to prepare the treatment plan precisely for saving a precious human life. The main

classification of primary brain tumors is based on their aggressiveness, which is benign and malignant. Benign tumor growth is very slow, has a distinct border, does not spread in surrounding tissue, and does not affect other body organs [5]. Malignant tumors grow quickly, have irregular borders, and spread in surrounding tissue and other body parts through metastasis [5].

1.1 Binary Classification of Brain Tumor: When a brain tumor is classified into two classes, such as tumor or non-tumor [6], high-grade glioma or low-grade glioma [7], benign or malignant, then it is called binary classification. This paper categorizes primary brain tumors in binary classes such as benign or malignant [8]. To test the proposed technique, glioma and pituitary tumors were chosen from Figshare dataset. The dataset contains three different classes of brain tumor MR images: 1426 glioma tumors, 930 pituitary tumors, and 708 meningioma tumors, based on their location. To perform the binary classification of brain tumors, glioma, and pituitary has been taken. Glioma tumors are mostly categorized as malignant in nature and pituitary tumors tend to be benign [9].

Pituitary develops more slowly than gliomas, they can nevertheless have an impact on bodily processes like growth, reproduction, and metabolism [10]. Malignant tumors and glioma tumors both have comparable shapes and sizes.

On the other hand, the shape and size of pituitary tumors are similar to benign tumors (Figure 1).

*1 Department of Electrical and Electronics Engineering,
B. P Mandal College of Engineering, Madhepura, Bihar
India, 852128;*

Email ID: hare.dbit@gmail.com

*2 Department of Computer Science and Engineering,
Government Engineering College, Munger, Bihar
India, 811202;*

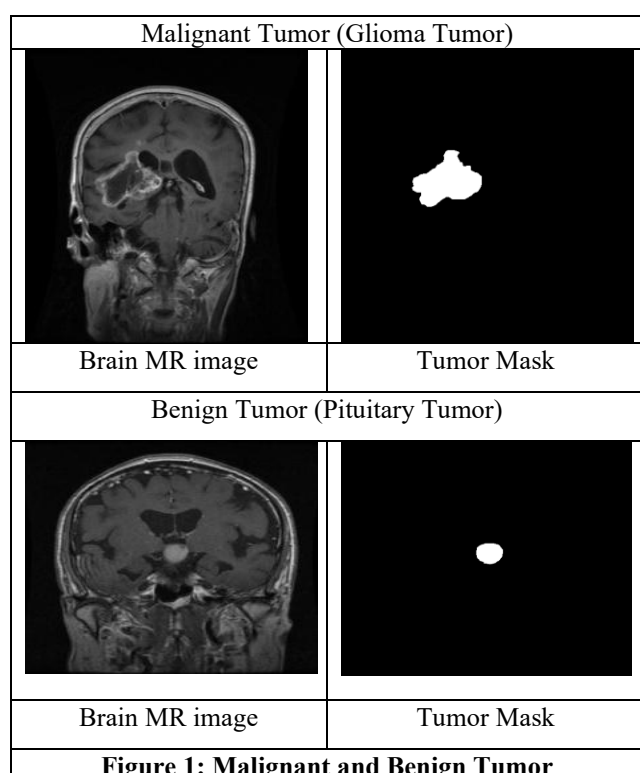
Email ID: gvnd.jha@gmail.com

*3 Department of Computer Science and Engineering,
Shri Phanishwar Nath Renu Engineering College, Araria,
Bihar, India, 854318;*

Email ID: krishnagac15@gmail.com

** Corresponding Author: Dr. Govind Kumar Jha*

E-mail Id: gvnd.jhal@gmail.com



Tumor mask shapes can help distinguish between benign and malignant tumors [11]. A benign tumor may turn malignant if it is not properly identified and treated on time [12]. Therefore, to reduce the mortality rate, early detection and classification of brain tumors are necessary.

1.2 Medical Imaging: The diagnosis of primary brain tumors is accomplished using several medical imaging modalities. In medical imaging, non-invasive diagnostic techniques are frequently employed [13]. These medical imaging methods include magnetoencephalography, computed tomography (CT), magnetoencephalography (EEG), positron emission tomography (PET), and magnetic resonance imaging (MRI), which is presently quite common [14]. MR imaging yields more useful information when detecting brain tumors than CT or ultrasound imaging and offers a model of the tumor's progression throughout therapy [15].

1.2.1 Magnetic Resonance Imaging (MRI): It provides different modalities [16] for diagnosing primary brain tumors. Dynamic Contrast-Enhanced Magnetic Resonance Imaging (DCE-MRI), T1-weighted, T2-weighted, Fluid Attenuated Inversion Recovery, and diffusion-weighted magnetic resonance imaging provide higher-quality images with more in-depth and comprehensive views of tissue or organs. DCE-MRI sequence is taken by injecting Gadolinium before T₁ sequencing. Gadolinium is a chemical component that can recognize the border between the brain and the blood, and this image contains more intensity due to the shorter longitudinal relaxation time. Three different positional views (Sagittal, Coronal, and Transverse) are possible in MRI, giving prominent characteristics to classify the brain tumor precisely. This study classified primary brain tumors as benign or

malignant using T1-weighted Dynamic Contrast-Enhanced MR imaging.

This is how the remaining part of the paper is structured. Section 2 presents the current research on the categorization of primary brain tumors. Section 3 presents the rationale, while Section 4 details the materials and suggested methods. The output findings are presented in Section 5. Section 6 wraps up the work done on this paper and outlines its future directions.

2. Literature Review

In machine learning algorithms, feature extraction and reduction are crucial steps before classifying brain tumors. Over the previous two decades, the diagnosis of brain tumors has been improved through computer-aided systems. Researchers have proposed various methods of classifying brain tumors. The related work of the researchers is discussed in this section.

Papageorgiou et al. introduced fuzzy cognitive maps and activation of the Hebbian algorithm to differentiate the tumor in low-grade and high-grade classes. They also identified the aggressive characteristics of the tumor [17]. Latif et al. introduced a combination of SVM, ANN, and ensemble classifiers, classifying the brain tumor in a binary class using GLCM features [18]. Singh and Kaur proposed an SVM classifier-based approach to classify brain tumor abnormality using GLCM texture features [19]. Jayachandran and Dhanasekaran proposed fuzzy SVM to classify the brain tumor in normal and abnormal classes using GLCM features and principal component analysis [20]. Ibrahim et al. used the Principal Component Analysis (PCA) for feature selection and classified the tumor as normal Edema and cancerous using a back propagation neural network [21]. Sudha et al. proposed grading the brain tumor through a BPNN classifier and extracting the features through GLCM and GLRM [22]. Sharma et al. proposed a binary classification of brain tumors by taking GLCM texture features and a Naive Bayes classifier [23]. Skogen et al. introduced a technique in which glioma tumors classify as low-grade glioma and high-grade glioma using filtration and FOSTF [24]. Sachdeva et al. extracted the shape, intensity, and texture features of MR images of brain tumors to classify primary and secondary brain tumors through SVM and ANN classifiers [25]. Hseih et al. proposed a global histogram and local texture-based feature extraction to classify low-grade glioma and high-grade glioma with the help of an ANN classifier [26]. Minz and Mahobiya proposed a model using GLCM features and an Adaboost classifier to classify the tumor as normal and abnormal [27]. Ari and Hanbay extracted intensity features to classify tumors as benign or malignant through ELM and SVM classifiers [28]. Alqasemi et al. introduced a binary classification of brain tumors with SVM classifier by using GLCM and statistical-based features [29].

The earlier works demonstrate how specific handcrafted texture features of magnetic resonance images are applied for the binary classification of brain cancers. The textural features of MR images are crucial in differentiating benign from malignant brain tumors. The goal is to improve the classification performance using these extracted texture features of MR images.

The paper proposes a methodology that uses seven handcrafted texture feature models, Gabor 2D filter, HTF, ECTF, FOSTF, LBPTF, DTTF, and STF. The proposed work examines the influence of texture features.

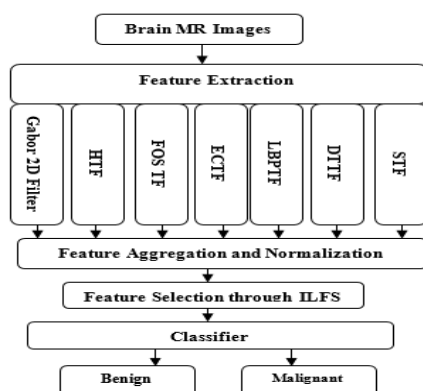
- Tanh-based normalization technique is used to normalize the extracted texture features.
- The ILFS technique is used to rank the normalized features.
- The proposed model is compared with different supervised classifier.

3. Motivation

One of the most important aspects of diagnosing brain cancer is the detection of brain tumors. The survival rates of patients quickly rose from 49% to 69% [30] after advancements in the field of non-invasive diagnosis techniques. For finding a brain tumor, MR images are better options than other medical imaging methods [15]. To save a priceless human life, it is crucial to correctly classify brain tumors after identification because incorrect classifications increase the chance of death. There are over 120 different forms of brain tumors, according to the World Health Organization (WHO) [31]. Malignant tumors are more aggressive, have a rapid growth rate, and are cancerous, whereas benign tumors are slow-growing, low-aggressive, and non-cancerous [32]. The texture features of MR images, which must be obtained accurately for efficient diagnosis, are mainly responsible for brain tumor classification.

4. Materials and Methodology

More effective therapies are available for patients with brain tumors if they are classified early. It has been shown that different texture models significantly influence brain tumour categorization; hence, seven texture models have been studied to reach this goal in the present work. Since not all features will be on the same scale, feature normalisation must be performed before applying any feature selection method. In this study, the retrieved features are rescaled with the use of Tanh-based normalisation techniques. As processing all possible features would take too much time and effort, the feature set is narrowed even further. The ILFS method simplifies things by picking out the features that actually matter to boost classification precision. The performance is analyzed with a Decision Tree, Discriminant, k-NN, Ensemble, and SVM classifiers. The block diagram of the proposed work is shown in figure 2.



4.1 Dataset Description: The dataset is publicly available on www.figshare.com, uploaded by Cheng et al. [33]. The set of images includes 3064 T1 contrast-enhanced MR scans of 233 people who had meningioma, pituitary tumors, and brain cancers. To assess the effectiveness of the proposed work, 930 images of patients with pituitary tumors and 1426 photographs of patients with glioma tumors are collected. These brain magnetic resonance imaging (MRI) scans are offered in the coronal, sagittal, and axial positioning views. The MR pictures of the brain, patient ID, tumor label, and details of the tumor mask (ground truth) are all included in the MAT files.

For the binary classification of brain tumor (Malignant and Benign), 1426 glioma tumor and 930 pituitary tumor has been taken. The glioma tumor is more aggressive and having similar properties as malignant tumor [34], [35]. The aggressive nature and growth characteristics is similar as benign [10], [36]. Grade I & II meningioma tumor are benign, but grade III meningioma tumor is malignant [37]. Due to this reason, 708 meningioma tumors are not considered for binary classification.

4.2 Feature Extraction: The patterns that can be observed in an image and provide significant information are called features. The most important step in any pattern recognition program is feature extraction as accuracy relies on selecting appropriate features. The presence of tumors in cerebrum-dense brain areas and their overlapping appearance characteristics make them difficult to classify. Therefore, a combination of seven texture models was used to extract the features of each suspicious region. The spatial distribution of grey levels around an image that is known as a texture feature. The texture characteristics describe the structural organization of the items in that image and their interactions with their environment. Texture traits can distinguish between malignant and normal tissues that cannot be immediately seen, and texture analysis offers strong discriminating characteristics related to variability patterns [38]. For feature extraction employing all suspicious areas from MR images of brain tumors, the suggested technique takes into account the texture characteristics of HTF, ECTF, FOSTF, LBPTF, DTTF, and STF in addition to the Gabor 2D filter.

4.2.1 Gabor 2D Filter: Mean amplitude and square energy are two textural features for grayscale photographs that Dennis Gabor presented [39]. A linear filter called the Gabor filter is used to analyze the texture of an image. In essence, it examines if a certain direction exists in a small area surrounding the analysis point or region [40]. Texture features with the Gabor 2D filter have been used for brain classification.

4.2.2 Haralick Texture Feature (HTF): Haralick et al. introduced the application of the Gray-Level Co-Occurrence Matrix (GLCM) and texture features, which are most widely used by selecting prominent features [41]. HTF is a significant feature used in diagnosing and classifying brain tumors. HTF are computed from GLCM for texture analysis to describe the textural characteristics of brain images. GLCM is a second-order statistic that defines

relationships between different tonal intensities for specific directions and distances [42]. The features are computed at a distance $d = 1$ to 4 for four directions, 0, 45, 90, and 135. HTF are extracted for binary and multiclass brain tumor classification.

4.2.3 Edge Continuity Texture Feature (ECTF): Susan et al. proposed an edge continuity based feature extraction method for the edges of a natural image with direction and angle specified [43]. Edge continuity features are shape features that express the appearance of the contour of an object by measuring location coherence between pixels. It follows four main orientations and encloses eight edge continuity characteristics that can describe a silhouette or pattern effectively. Thus, the object contour is given as a sum of all four Edge direction features and all four Edge direction continuity features [44]. Edge Continuity Section features are used to detect and categorize brain tumors.

4.2.4 First-order Statistical Texture Feature (FOSTF): The features are extracted by utilizing first-order statistical moments such as standard deviation, mean, kurtoses and skewness with grey-level histogram of images [45]. The mean represents the average intensity of pixel in an image, the standard deviation measures the contrast level in an image, skewness measures symmetry and kurtosis records relative flatness [45].

4.2.5 Local Binary Pattern Texture Feature (LBPTF): Ojala et al. proposed an algorithm for the extraction of local binary pattern features [47]. An edge detector using the signs of differences between neighbouring and central pixels makes binary codes by thresholding the pixel value at each point in the image to their neighbor pixels using the center point. Based on this threshold value, this is considered a binary map such that the neighboring pixel changes to 1 or 0. One is represented by the higher value and zero with the lower value. A histogram is used to represent the frequency values of binary patterns. The number of histogram bins is equal to the number of pixels used in local binary pattern calculations.

4.2.6 Difference Theoretic Texture Features (DTTF): It is a textural parameter that describes feature based on the absolute differences of global and local gray level in combination with associated probability values from signed gray level difference histogram. This quantity is computed pixelwise and then averaged over all pixels in the image for scale, rotation, and illumination [48]. Therefore, the three-dimensional feature subset of local horizontal difference, local vertical difference and local diagonal difference is acquired to calculate the magnitude of local difference. It implies that 11 features are extracted from each texture image.

4.2.7 Spectral Texture Feature (STF): Feng and Liu proposed Fourier spectrum-based spectral texture analysis for measuring textural features [49]. The Fourier spectrum can be written in the polar coordinates $S(r, \theta)$, where S is the spectrum function for the image and r, θ are radius and angle in the polar coordinate system [50].

4.3 Feature Normalization: Feature normalization is a process that rescales or modifies raw data so that each feature has an equal contribution. Tanh-based normalization was suggested by Hampel et al., where Hampel estimator-based data transformation was used [51]. The main advantage of Tanh-based normalization is that its negative inputs are strongly negative, and zero inputs are always mapped near zero [52]. In this normalization method, each instance is represented as:

$$X'_{i,n} = 0.5 \left\{ \tanh \left(0.01 \left(\frac{X_{i,n} - \mu_i^h}{\sigma_i^h} \right) \right) + 1 \right\} \quad (1)$$

σ^h is the standard deviation, and μ^h is the mean of the Hampel estimator. The estimators depend on influence parameters (ϕ), which can be expressed as follows:

$$\phi(\vartheta) = \begin{cases} \vartheta & 0 \leq \vartheta \leq u_1, \\ u_1 \times \text{sign}(\vartheta) & u_1 \leq \vartheta \leq u_2, \\ u_1 \times \text{sign}(\vartheta) \times \frac{u_3 - |\vartheta|}{pu_3 - u_2} & u_2 \leq \vartheta \leq u_3, \\ 0 & |\vartheta| > u_3, \end{cases} \quad (2)$$

$\vartheta_{i,n} = X_{i,n} - \text{med}(X_i)$, $\text{sign}(\vartheta) = 1$ for $\vartheta \geq 0$ and $\text{sign}(\vartheta) = -1$ for $\vartheta < 0$.

The above function provides decreasing influence values at the bottom of the distributions while estimating the scale parameter and location. The results show that it is unaffected by outliers.

4.4 Feature Selection: Selecting important features while deleting redundant and irrelevant features is known as feature selection. This paper uses the ILFS [53] to identify the relevant features that show a better classification performance due to the application of Probabilistic Latent Semantic Analysis (PLSA). The weights may be derived using the PLSA method using probability co-occurrences among features and tokens. This technique is employed in three steps: the first step is pre-processing, the second is weighting the graph, and the last is ranking the features. The selection of features may be wrapper or filter techniques. The entire process of this feature selection is discussed in detail as follows:

4.4.1 Co-occurrence of Graph Weighting: The weight of training data is calculated as per their degree of importance. Tentative probabilities of factor/features and token/features are calculated. Exceptional maximization is used for parameter optimization.

4.4.2 Probabilistic IFS: Expansion of the path to infinity and geometric series is calculated from the matrix obtained in the previous steps. Galfandi's formula [54] is used to obtain the rank of the features:

$$C = (1 - rB)^{-1} - I \quad (3)$$

Here, B is the matrix obtained by the co-occurrence of graph weighting, I denotes the identity matrix, and r is expressed as

$$r = \frac{1}{\max(\text{eigen value } [B])} \quad (4)$$

By adding the matrix dimensions, the path length energy score is calculated. At last, the rank of the feature is evaluated.

The ILFS method does not automatically select the appropriate features, so the number of prominent features is selected manually. The approach adopted in this work is

focused on picking an appropriate range and a specific value. The process is repeated until a suitable set of characteristics provides the highest accuracy value. 399 texture features have been retrieved for this study.

Using the SVM classifier, the desired number of features to be chosen ranges from 150 to 250, with a gap of 10. Out of these, 190 features have resulted in better accuracy in these sets. Further, a new feature subset has been created for the features from 190 to 210, and in this set, 200 features have yielded the best accuracy.

4.5 Classification: The classifiers that the researchers have widely used are Decision Tree classifier, Discriminant classifier, k-NN classifier, Ensemble classifier, SVM classifier, Naive Bayes classifier, Artificial neural network classifier, and probabilistic neural network classifier. So, this paper considers the following classifiers to evaluate and compare the results with the proposed methods.

4.5.1 Decision Tree: The tree-based classifier frequently breaks down the most complicated issue into a simple method [55]. It employs input training characteristics, in which each branch of a particular tree contributes to the outcome. A decision tree may readily be converted into a collection of rules the reader can understand [56].

4.5.2 Discriminant Classifier: This classifier anticipates diverse Gaussian circulations among different classes [57]. There are two types of discriminant classifiers, linear and quadratic discriminant. In this paper, a quadratic discriminant classifier is used to evaluate the performance of the proposed work.

4.5.3 k- Nearest Neighbours (k-NN) Classifier: It is an instance-based classifier that predicts new elements in a test dataset, based on K-labelled points in the training set. Test data is classified based on its similarity with the training data. The test data belongs to one of the training data's class labels [58]. It's easier to understand the k-NN classifier. The inbuilt noise reduction helps in classifying with an accuracy [59]. Performance of these classifiers has been assessed using the Weighted k-NN, Fine k-NN and Median k-NN.

4.5.4 Ensemble Classifier: It is a collection of individual classifiers that work together to train a data set [60]. It is based on manipulating the training parameters, error function, feature space, output labels, clustering, and training pattern manipulation. Ensemble bagged trees and Ensemble Subspace Discriminant classifier is used to evaluate the performance of this proposed work.

4.5.5 Support Vector Machine (SVM) Classifier: The SVM classifier tries to separate boundaries, which act as building blocks of this classifier. It uses this kernel function and hyperplane. This relies on a statistical learning theory and is one of Vapnik's computational approaches [61]. If the extracted characteristics are inseparable, nonlinear kernel modifications are utilized. The cubic SVM classifier has been well implemented for large-dimensional spaces and can also process nominal and continuous data [62]. It considers the performance evaluation of the proposed

method with Linear SVM, Quadratic SVM, and Cubic SVM classifiers.

4.6 Performance evaluation Metrics: The effectiveness of the proposed techniques for brain tumors is examined through different parameters calculated using a confusion matrix. The performance of the proposed method is evaluated by performance evaluation parameters such as sensitivity, specificity, precision, MCC, Error rate, F1-Score, and accuracy.

4.6.1 Precision: It represents the proximity of the two evaluated values to each other, and is calculated as:

$$\frac{TP}{FP + TP} \quad (5)$$

Where TP is true positive and FP is false positive.

4.6.2 Sensitivity: It represents the capacity of a classifier to classify brain tumors correctly, and it is calculated as:

$$\frac{TP}{TP + FN} \quad (6)$$

Where TP is true positive and FN is false negative.

4.6.3 Specificity: It represents the classifier's ability to classify the brain tumor precisely, and calculated as:

$$\frac{TN}{FP + TN} \quad (7)$$

Where TN is true negative and FP is false positive.

4.6.4 F1-Score: It is taken to identify the test accuracy of a classifier, and calculated as:

$$\frac{2 \times (Precision \times Specificity)}{(Precision + Specificity)} \quad (8)$$

4.6.5 Error Rate: It is defined as the ratio of false prediction to the whole dataset, and formulated as:

$$\frac{FP + FN}{TP + FP + TN + FN} \quad (9)$$

4.6.7 Mathew Correction Coefficient: It is defined as, the superiority evaluation of classification, and calculated as:

$$\frac{(TP \times TN) - (FP \times FN)}{\sqrt{(TP + FP)(TP + FN)(TN + FP)(TN + FN)}} \quad (10)$$

4.6.7: Accuracy: It is used to determine the classes of brain tumors accurately, and is represented as:

$$\frac{TP + TN}{TP + FP + TN + FN} \quad (11)$$

5. Results and Discussion: In this paper, we propose a technique for binary classification of primary brain tumors (HGG and LGG) from magnetic resonance images of the brain. We consider all the brain magnetic resonance images of 1426 gliomas and 930 pituitary tumors available in the Figshare dataset to evaluate the performance of the proposed methodology. The suspicious regions in the MR images are extracted using texture features to classify the tumor as benign or malignant.

Seven different handcrafted texture models are used in this work to extract texture features from suspicious areas: the Gabor 2D filter, HTF, ECTF, FOSTF, LBPTF, DTTF, and STF. Extracted textural features for locations suspected of

harboring gliomas and pituitary tumors total 399 (see Table 1).

Hand-Crafted Texture Model	Extracted Feature (399)	Feature Selected (200)
Gabor 2D Filter	60	28
HTF	14	8
ECTF	8	8
FOSTF	4	2
LBPTF	59	55
DTTF	11	2
STF	243	97

The Tanh-based normalization method is applied to normalize the extracted feature set. After normalizing the feature set, the ILFS method is used to rank the normalized features. The top 200 relevant features, including every extracted handcrafted texture feature, give the best binary classification of a brain tumor as benign or malignant.

Experiments have been carried out on a system with an Intel Core i7 with a 2.40 GHz processor and 8.00 GB of memory running under Windows 10 Pro. A 10-fold cross-validation procedure is adopted to evaluate the results using the Decision Tree, Discriminant, k-NN, Ensemble, and SVM classifiers. The proposed work has been compared with five classifiers and their variants using evaluation parameters such as precision, sensitivity, specificity, F1-score, error rate, MCC, and classification accuracy.

The proposed work gives a model for the binary classification of primary brain tumors into malignant and benign. Performance parameters of the classifier are evaluated with the help of the confusion matrix of the classifiers..

Table 2: Performance evaluation of classifiers with selected features

Classifier	CT	QD	k-NN 1	k-NN 2	k-NN 3	ESD	EBT	SVM-1	SVM-2	Cubic SVM
Precision (%)	M 93.16	82.88	98.38	98.43	99.16	99.64	99.08	99.37	99.78	99.64
	B 91.18	86.12	93.76	96.23	98.60	95.26	93.65	97.41	95.16	99.03
Sensitivity (%)	M 94.28	90.16	96.03	97.36	99.08	96.59	95.99	98.33	96.93	99.33
	B 92.07	76.65	97.43	97.60	98.70	99.43	98.32	98.90	99.66	99.46
Specificity (%)	M 92.07	76.65	97.43	97.60	98.70	99.43	98.32	98.90	99.66	99.46
	B 94.28	90.16	96.03	97.36	99.08	96.59	95.99	98.33	96.93	99.33
F1-Score	M 0.9338	0.7964	0.9790	0.9801	0.9893	0.9953	0.9865	0.9923	0.9971	0.9984
	B 0.9270	0.8809	0.9488	0.9689	0.9883	0.9611	0.9480	0.9786	0.9603	0.9917

M: Malignant, B: Benign, CT: Complex Tree, QD: Quadratic Discriminant, k-NN 1: Median k-NN, k-NN 2: Weighted k-NN, k-NN 3: Fine k-NN, ESD: Ensemble Subspace Discriminant, EBT: Ensemble Bagged Tree, SVM-1: Quadratic SVM, SVM-2: Fine Gaussian SVM

The classifier's performance based on precision, sensitivity, specificity, and the F1-Score of a benign and malignant tumor is shown in Table 2.

Three different k-NN classifiers are tested; however, the Fine k-NN classifiers get the highest accuracy at 98.9 percent. The ensemble subspace discriminant outperforms the other ensemble classifier, with an accuracy of 97.9% when classifying a brain tumour. In addition, three distinct SVM classifier variations have been used to solve the problem of classifying the brain cancers. When compared to other classifiers, the cubic SVM classifier has the highest performance and accuracy (99.4%).

According to Figure 3, the higher value of classification accuracy and the higher MCC value achieved through the cubic SVM classifier show its superiority among all classifiers.

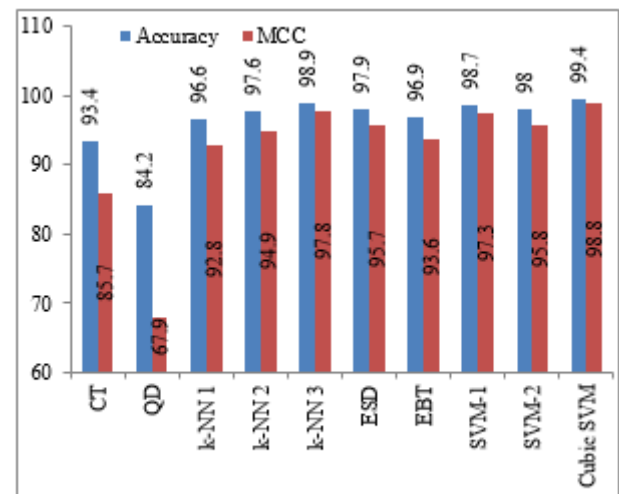


Figure 3: Classifier Performance

The error rate of the classifier is shown in figure 4. The lowest value of error rates indicates the better performance of the classifier. Quadratic discriminant classifiers perform worst based on error rate. All these values of the cubic classifier show that their performance is better than other classifiers.

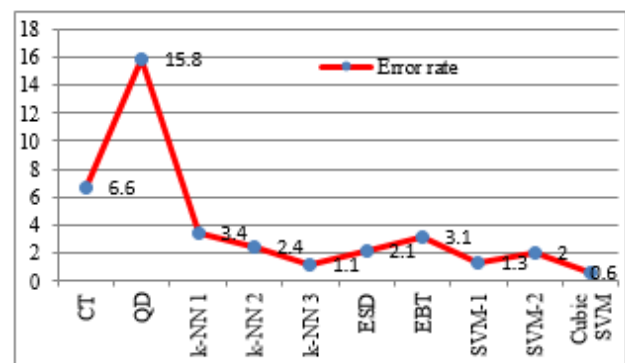


Figure 4: Error rate of classifiers

The result of the proposed work is also compared with different related methods in Table 3 for achieving best performance. In this review, accuracy is the universally employed performance metric in all state-of-the-art methods to measure the effectiveness of the proposed method. Bahadure et al. applied the SVM classifier based on a combination of biologically inspired Berkeley wavelet subbands to the binary class grading of brain tumors. Results: 201 MR images of brain tumors were captured and then the system was trained on 67 normal and 134 abnormal brain tumor MR images with accuracy in classification ranging to 95%. Shree and Kumar extracted the GLCM features of 650 brain tumor MR images and achieved 95% binary classification accuracy using a probabilistic neural network classifier. Ullah et al. proposed binary classification through the advanced deep neural network with 95.8% classification accuracy and features extracted from 71 brain tumor MR images by discrete wavelet transform. Ansari et al. extracted the GLCM and DWT features of 200 T-1 contrast-enhanced MR images of brain tumors. The SVM classifier was taken with PCA to achieve 98.91% binary classification accuracy. Alqasemi et al. took

the Kaggle data set containing 253 binary class MR images of brain tumors. Alqasemi et al. extracted the GLCM feature and achieved 98% binary classification accuracy by using the SVM classifier. Preethi and Aishwarya extracted GLCM features from 20 MR images of brain tumors, and a deep neural network classifier was taken to classify the brain tumor in binary class with 92% accuracy. The comparisons of the proposed methodology with other state-of-the-art methods indicate that it surpasses all state-of-the-art techniques and gives the highest binary classification accuracy.

Table 3: A Comparison of state-of-the-art methods for primary brain tumor classification

Authors	Texture Features / Classifier used	Database	Accuracy (%)
Bahadure et al. (2017) [63]	BWT+SVM	T2-weighted brain images, 67 normal and 134 abnormal	95.00
Shree & Kumar (2018) [38]	GLCM+PNN	650 MR images DIACOM	95.00
Ullah et al. (2020) [64]	DWT + Feed-Forward Neural Network	71 MR Images	95.80
Ansari et al. (2020) [65]	DWT+PCA+GLCM+SVM	T1-weighted CE-MRI, 140 tumors affected, 60 normal	98.91
Alqasemi et al. (2021) [29]	GLCM + SVM	Kaggle Dataset (98 Normal and 155 abnormal MR Images)	98.00
Preethi & Aishwarya (2021) [66]	GLCM+DNN	20 MR Images	92.00
Rao et al. (2022) [67]	EQPE + Entropy ranking + k-NN classifier	TCIA 800 MR images	92.5
Hameed et al. (2022) [68]	GLCM+CNN	Benign-164 and Malignant-170	96.2
Gupta et al. [69]	VGG16	Kaggle Dataset (98 Normal and 155 abnormal MR Images)	96
Proposed Methodology	Normalized Texture Features + Cubic SVM	T1-weighted CE-MRI, 1426 gliomas, and 930 pituitary tumors	99.40

6. Conclusion

The accurate classification of the primary brain tumor is crucial for initiating early treatment and preserving precious human life since it has a significant impact on lowering the mortality rate of brain tumor patients. The main goal of this proposed method is to develop an efficient binary classification of primary brain tumor with high accuracy. The texture features of brain MR images are extracted through the Gabor 2D filter, HTF, ECTF, FOSTF, LBPTF, DTF and STF and aggregate to prepare a set of texture feature. Tanh-based normalization is taken to normalize these extracted features to improve the efficiency of the proposed system. After that, the infinite latent features selection is used to rank the relevant features. The top 200 ranked features are selected and evaluated with classifiers. Cubic SVM classifier gives high sensitivity, the best F1-score, and a low error rate compared with other classifiers. It provides 99.4% primary brain tumor binary classification accuracy with 10-fold cross-validation. In the future, multiclass classification can be proposed to classify the malignant tumor as grades I, II, III, and IV to make the treatment plan precisely.

References

- [1] K. Dimililer and A. İlhan, "Effect of Image Enhancement on MRI Brain Images with Neural Networks," *Procedia Comput. Sci.*, vol. 102, pp. 39–44, Jan. 2016, <https://doi.org/10.1016/j.procs.2016.09.367>.
- [2] S. R. Gunasekara, H. N. T. K. Kaldera, and M. B. Dissanayake, "A Systematic Approach for MRI Brain Tumor Localization and Segmentation Using Deep Learning and Active Contouring," *J. Healthc. Eng.*, vol. 2021, pp. 1–13, Feb. 2021, <https://doi.org/10.1155/2021/6695108>.
- [3] A. Dasgupta, T. Gupta, and R. Jalali, "Indian data on central nervous tumors: A summary of published work," *South*

- Asian J. Cancer*, vol. 05, no. 03, pp. 147–153, Jul. 2016, <https://doi.org/10.4103/2278-330X.187589>.
- [4] Q. T. Ostrom, G. Cioffi, H. Gittleman, N. Patil, K. Waite, C. Kruchko, and J. S. Barnholtz-Sloan, "CBTRUS statistical report: Primary brain and other central nervous system tumors diagnosed in the United States in 2012–2016," *Neuro. Oncol.*, vol. 21, no. Supplement_5, pp. v1–v100, Nov. 2019, <https://doi.org/10.1093/neuonc/noz150>.
- [5] A. Patel, "Benign vs Malignant Tumors," *JAMA Oncology*, vol. 6, no. 9, p. 1488, 2020, <https://doi.org/10.1001/jamaoncol.2020.2592>.
- [6] R. Mohan, K. Ganapathy, and A. Rama, "Brain tumor classification of magnetic resonance images using a novel CNN-based medical image analysis and detection network in comparison with AlexNet," *J. Popul. Ther. Clin. Pharmacol.*, vol. 29, no. 1, pp. e97–e108, 2022, <https://doi.org/10.47750/jptcp.2022.898>.
- [7] G. Latif, D. N. F. A. Iskandar, J. M. Alghazo, and N. Mohammad, "Enhanced MR Image Classification Using Hybrid Statistical and Wavelets Features," *IEEE Access*, vol. 7, pp. 9634–9644, 2019, <https://doi.org/10.1109/ACCESS.2018.2888488>.
- [8] M. A. Khan, I. Ashraf, M. Alhaisoni, R. Damaševičius, R. Scherer, A. Rehman, and S. A. C. Bukhari, "Multimodal Brain Tumor Classification Using Deep Learning and Robust Feature Selection: A Machine Learning Application for Radiologists," *Diagnostics*, vol. 10, no. 8, p. 565, Aug. 2020, <https://doi.org/10.3390/diagnostics10080565>.
- [9] K. D. Miller, Q. T. Ostrom, C. Kruchko, N. Patil, T. Tihan, G. Cioffi, H. E. Fuchs, K. A. Waite, A. Jemal, R. L. Siegel, and J. S. Barnholtz-Sloan, "Brain and other central nervous system tumor statistics, 2021," *CA. Cancer J. Clin.*, vol. 71, no. 5, pp. 381–406, Sep. 2021, <https://doi.org/10.3322/caac.21693>.
- [10] R. Shrwan and A. Gupta, "Classification of Pituitary Tumor and Multiple Sclerosis Brain Lesions through Convolutional Neural Networks," *IOP Conf. Ser. Mater. Sci. Eng.*, vol. 1049, no. 1, p. 012014, 2021, <https://doi.org/10.1088/1757-899x/1049/1/012014>.
- [11] D. N. George, H. B. Jehlol, and A. S. A. Oleiwi, "Brain tumor detection using shape features and machine learning algorithms," *Int. J. Sci. Eng. Res.*, vol. 6, no. 12, pp. 454–459, 2015.
- [12] K. Herholz, K. Langen, C. Schiepers, and M. James, "NIH Public Access," vol. 42, no. 6, pp. 356–370, 2014, <https://doi.org/10.1053/j.semnuclmed.2012.06.001.Brain>.
- [13] Y. Abdallah and Y. Mohamed, "History of medical imaging," *Arch. Med. Heal. Sci.*, vol. 5, no. 2, p. 275, 2017, https://doi.org/10.4103/amhs.amhs_97_17.
- [14] H. Kasban, M. A. M. El-Bendary, and D. H. Salama, "A Comparative Study of Medical Imaging Techniques," *Int. J. Inf. Sci. Intell. Syst.*, vol. 4, no. 2, pp. 37–58, 2015.
- [15] J. Seetha and S. S. Raja, "Brain tumor classification using convolutional neural networks," *Biomed. Pharmacol. J.*, vol. 11, no. 3, pp. 1457–1461, Sep. 2018, <https://doi.org/10.13005/bpj/1511>.
- [16] V. P. B. Grover, J. M. Tognarelli, M. M. E. Crossey, I. J. Cox, S. D. Taylor-Robinson, and M. J. W. McPhail, "Magnetic Resonance Imaging: Principles and Techniques: Lessons for Clinicians," *J. Clin. Exp. Hepatol.*, vol. 5, no. 3, pp. 246–255, 2015, <https://doi.org/10.1016/j.jceh.2015.08.001>.
- [17] E. I. Papageorgiou, P. P. Spyridonos, D. T. Glotsos, C. D. Stylios, P. Ravazoula, G. N. Nikiforidis, and P. P. Groumpos, "Brain tumor characterization using the soft computing technique of fuzzy cognitive maps," *Appl. Soft Comput. J.*, vol. 8, no. 1, pp. 820–828, 2008, <https://doi.org/10.1016/j.asoc.2007.06.006>.
- [18] G. Latif, S. B. Kazmi, M. A. Jaffar, and A. M. Mirza, "Classification and Segmentation of Brain Tumor Using

Texture Analysis,” in *Recent Advances In Artificial Intelligence, Knowledge Engineering And Data Bases*, 2010, pp. 147–155.

- [19] D. Singh and K. Kaur, “Classification of Abnormalities in Brain MRI Images Using GLCM, PCA and SVM,” *Int. J. Eng. Adv. Technol.*, vol. 1, no. 6, pp. 243–248, 2012.
- [20] A. Jayachandran and R. Dhanasekaran, “Brain Tumor Detection and Classification of MR Images Using Texture Features and Fuzzy SVM Classifier,” *Res. J. Appl. Sci. Eng. Technol.*, vol. 6, no. 12, pp. 2264–2269, Jul. 2013, <https://doi.org/10.19026/rjaset.6.3857>.
- [21] W. H. Ibrahim, A. A. A. Osman, and Y. I. Mohamed, “MRI brain image classification using neural networks,” *Proc. - 2013 Int. Conf. Comput. Electr. Electron. Eng. 'Research Makes a Differ. ICCEEE 2013*, pp. 253–258, 2013, <https://doi.org/10.1109/ICCEEE.2013.6633943>.
- [22] B. Sudha, P. Gopikannan, Shenbagarajan, and C. Balasubramanian, “Classification of brain tumor grades using neural network,” *Lect. Notes Eng. Comput. Sci.*, vol. 1, pp. 567–571, 2014.
- [23] Sharma et al., “Brain Tumor Detection based on Machine Learning Algorithms,” *International Journal of Computer Applications INDIA*, vol. 103, no. 1, pp. 7–11, 2014, [Online]. Available: www.ijcaonline.org
- [24] K. Skogen, A. Schulz, J. B. Dormagen, B. Ganeshan, E. Helseth, and A. Server, “Diagnostic performance of texture analysis on MRI in grading cerebral gliomas,” *Eur. J. Radiol.*, vol. 85, no. 4, pp. 824–829, Apr. 2016, <https://doi.org/10.1016/j.ejrad.2016.01.013>.
- [25] J. Sachdeva, V. Kumar, I. Gupta, N. Khandelwal, and C. K. Ahuja, “A package-SFERCB-“Segmentation, feature extraction, reduction and classification analysis by both SVM and ANN for brain tumors”,” *Appl. Soft Comput. J.*, vol. 47, pp. 151–167, 2016, <https://doi.org/10.1016/j.asoc.2016.05.020>.
- [26] K. L. C. Hsieh, C. M. Lo, and C. J. Hsiao, “Computer-aided grading of gliomas based on local and global MRI features,” *Comput. Methods Programs Biomed.*, vol. 139, pp. 31–38, 2017, <https://doi.org/10.1016/j.cmpb.2016.10.021>.
- [27] A. Minz and C. Mahobiya, “MR image classification using adaboost for brain tumor type,” *Proc. - 7th IEEE Int. Adv. Comput. Conf. IACC 2017*, pp. 701–705, 2017, <https://doi.org/10.1109/IACC.2017.0146>.
- [28] A. Ari and D. Hanbay, “Deep learning based brain tumor classification and detection system,” *TURKISH J. Electr. Eng. Comput. Sci.*, vol. 26, no. 5, pp. 2275–2286, Sep. 2018, <https://doi.org/10.3906/elk-1801-8>.
- [29] U. Alqasemi, M. Bamaleibd, and A. Al Baiti, “Classification of Brain MRI Tumor Images,” *Int. J. Eng. Res. Technol.*, vol. 10, no. 03, pp. 119–126, 2021.
- [30] A. Elmoufidi, K. EL Fahssi, S. Jai-Andaloussi, N. Madrane, and A. Sekkaki, “Detection of regions of interest’s in mammograms by using local binary pattern, dynamic k-means algorithm and gray level co-occurrence matrix,” in *2014 International Conference on Next Generation Networks and Services (NGNS)*, May 2014, pp. 118–123. <https://doi.org/10.1109/NGNS.2014.6990239>.
- [31] R. Banan and C. Hartmann, “The new WHO 2016 classification of brain tumors-what neurosurgeons need to know,” *Acta Neurochir. (Wien)*, vol. 159, no. 3, pp. 403–418, Mar. 2017, <https://doi.org/10.1007/s00701-016-3062-3>.
- [32] P. S. Shijin Kumar and V. S. Dharun, “A study of MRI segmentation methods in automatic brain tumor detection,” *Int. J. Eng. Technol.*, vol. 8, no. 2, pp. 609–614, 2016.
- [33] J. Cheng, W. Huang, S. Cao, R. Yang, W. Yang, Z. Yun, Z. Wang, and Q. Feng, “Enhanced performance of brain tumor classification via tumor region augmentation and partition,” *PLoS One*, vol. 10, no. 10, p. e0140381, Oct. 2015, <https://doi.org/10.1371/journal.pone.0140381>.
- [34] A. K. Altwairgi, S. Raja, M. Manzoor, S. Aldandan, E. Alsaeed, A. Balbaid, H. Alhussain, Y. Orz, A. Lary, and A. A. Alsharm, “Management and treatment recommendations for World Health Organization Grade III and IV gliomas,” *Int. J. Health Sci. (Qassim)*, vol. 11, no. 3, pp. 54–62, 2017, [Online]. Available: <http://www.ncbi.nlm.nih.gov/pubmed/28936153> <http://www.pubmedcentral.nih.gov/articlerender.fcgi?artid=PMC5604271>
- [35] Choksey et al., “Computed tomography in the diagnosis of malignant brain tumours: do all patients require biopsy?,” *J. of Neurology, Neurosurgery, Psychiatry*, vol. 52, pp. 821–825, 1989, <https://doi.org/10.1136/jnnp.52.7.821>.
- [36] P. U. Freda and S. L. Wardlaw, “Diagnosis and Treatment of Pituitary Tumors,” 1999. [Online]. Available: <https://academic.oup.com/jcem/article/84/11/3859/2864212>
- [37] R. A. Buerki, C. M. Horbinski, T. Kruser, P. M. Horowitz, C. D. James, and R. V. Lukas, “An overview of meningiomas,” *Futur. Oncol.*, vol. 14, no. 21, pp. 2161–2177, Sep. 2018, <https://doi.org/10.2217/fon-2018-0006>.
- [38] N. Varuna Shree and T. N. R. Kumar, “Identification and classification of brain tumor MRI images with feature extraction using DWT and probabilistic neural network,” *Brain Informatics*, vol. 5, no. 1, pp. 23–30, Mar. 2018, <https://doi.org/10.1007/s40708-017-0075-5>.
- [39] D. Gabor, “Theory of communication. Part 1: The analysis of information,” *J. Inst. Electr. Eng. - Part III Radio Commun. Eng.*, vol. 93, no. 26, pp. 429–441, Nov. 1946, <https://doi.org/10.1049/ji-3-2.1946.0074>.
- [40] M. R. Ismael and I. A. Qader, “Brain tumor classification via statistical features and back-propagation neural network,” in *2018 IEEE International Conference on Electro/Information Technology (EIT)*, May 2018, vol. 2018-May, pp. 0252–0257. <https://doi.org/10.1109/EIT.2018.8500308>.
- [41] R. M. Haralick, K. Shanmugam, and I. Dinstein, “Textural features for image classification,” *IEEE Trans. Syst. Man. Cybern.*, vol. SMC-3, no. 6, pp. 610–621, Nov. 1973, <https://doi.org/10.1109/TSMC.1973.4309314>.
- [42] D. Assefa, H. Keller, C. Ménard, N. Laperriere, R. J. Ferrari, and I. Yeung, “Robust texture features for response monitoring of glioblastoma multiforme on T1-weighted and T2-FLAIR MR images: a preliminary investigation in terms of identification and segmentation,” *Med. Phys.*, vol. 37, no. 4, pp. 1722–36, Apr. 2010, <https://doi.org/10.1118/1.3357289>.
- [43] S. Susan, P. Agrawal, M. Mittal, and S. Bansal, “New shape descriptor in the context of edge continuity,” *CAAI Trans. Intell. Technol.*, vol. 4, no. 2, pp. 101–109, Jun. 2019, <https://doi.org/10.1049/trit.2019.0002>.
- [44] S. R. Telrandhe, A. Pimpalkar, and A. Kendhe, “Detection of brain tumor from MRI images by using segmentation & SVM,” in *2016 World Conference on Futuristic Trends in Research and Innovation for Social Welfare (Startup Conclave)*, Feb. 2016, no. November 2018, pp. 1–6. <https://doi.org/10.1109/STARTUP.2016.7583949>.
- [45] R. C. Gonzalez and R. E. Woods, “Digital Image Processing,” *Pearson Int. Ed.*, vol. 3, pp. 1–976, 2002.
- [46] N. Aggarwal and R. K. Agrawal, “First and Second Order Statistics Features for Classification of Magnetic Resonance Brain Images,” *J. Signal Inf. Process.*, vol. 03, no. 02, pp. 146–153, 2012, <https://doi.org/10.4236/jsip.2012.32019>.
- [47] T. Ojala, “A Comparative Study of Texture Measures With Classification Based on Feature Distributions,” *Pattern Recognit.*, vol. 29, no. 1, pp. 51–59, 1996.
- [48] S. Susan and M. Hanmandlu, “Difference theoretic feature set for scale-, illumination- and rotation-invariant texture classification,” *IET Image Process.*, vol. 7, no. 8, pp. 725–732, Nov. 2013, <https://doi.org/10.1049/iet-ipr.2012.0527>.
- [49] C. Feng and Q. Liu, “A study of digital watermark algorithm based on HVS for halftone images,” *Adv. Mater. Res.*, vol. 174, pp. 127–131, 2011,

- <https://doi.org/10.4028/www.scientific.net/AMR.174.127>.
- [50] D. Kim, Y. Lee, B. Ku, and H. Ko, "Crowd density estimation using multi-class adaboost," in *2012 IEEE Ninth International Conference on Advanced Video and Signal-Based Surveillance*, Sep. 2012, pp. 447–451. <https://doi.org/10.1109/AVSS.2012.31>.
 - [51] F. R. Hampel, E. M. Ronchetti, P. J. Rousseeuw, and W. A. Stahel, *Robust Statistics*. Wiley, 2005. <https://doi.org/10.1002/9781118186435>.
 - [52] C. Nwankpa, W. Ijomah, A. Gachagan, and S. Marshall, "Activation Functions: Comparison of trends in Practice and Research for Deep Learning," pp. 1–20, Nov. 2018, <https://doi.org/doi.org/10.48550>.
 - [53] G. Roffo, S. Melzi, U. Castellani, and A. Vinciarelli, "Infinite Latent Feature Selection: A Probabilistic Latent Graph-Based Ranking Approach," *Proc. IEEE Int. Conf. Comput. Vis.*, vol. 2017-Octob, pp. 1407–1415, 2017, <https://doi.org/10.1109/ICCV.2017.156>.
 - [54] F. Melgani and L. Bruzzone, "Classification of hyperspectral remote sensing images with support vector machines," *IEEE Trans. Geosci. Remote Sens.*, vol. 42, no. 8, pp. 1778–1790, Aug. 2004, <https://doi.org/10.1109/TGRS.2004.831865>.
 - [55] D. T. Larose, *An Introduction to Data Mining The CRISP-DM*. 1999.
 - [56] L. Rokach and O. Maimon, *Data Mining With Decision Trees*. 2005.
 - [57] T. Ramayah, N. H. Ahmad, H. A. Halim, S. Rohaida, M. Zainal, and M. Lo, "Discriminant analysis : An illustrated example," *African J. Bus. Manag.*, vol. 4, no. 9, pp. 1654–1667, 2010.
 - [58] D. T. Larose and C. D. Larose, *DISCOVERING KNOWLEDGE IN DATA An Introduction to Data Mining Second Edition Wiley Series on Methods and Applications in Data Mining*. 2014.
 - [59] S. J. Delany and P. Cunningham, "An Analysis of Case-Base Editing in a Spam Filtering System," in *Lecture Notes in Computer Science (including subseries Lecture Notes in Artificial Intelligence and Lecture Notes in Bioinformatics)*, vol. 3155, 2004, pp. 128–141. https://doi.org/10.1007/978-3-540-28631-8_11.
 - [60] R. Polikar, "Ensemble based systems in decision making," *IEEE Circuits Syst. Mag.*, vol. 6, no. 3, pp. 21–44, 2006, <https://doi.org/10.1109/MCAS.2006.1688199>.
 - [61] C. Cortes and V. Vapnik, "Support-vector networks," *Mach. Learn.*, vol. 20, no. 3, pp. 273–297, Sep. 1995, <https://doi.org/10.1007/BF00994018>.
 - [62] P. Drotar and Z. Smekal, "Comparative Study of Machine Learning Techniques for Supervised Classification of Biomedical Data," *Acta Electrotech. Inform.*, vol. 14, no. 3, pp. 5–10, 2014, <https://doi.org/10.15546/aei-2014-0021>.
 - [63] N. B. Bahadure, A. K. Ray, and H. P. Thethi, "Image Analysis for MRI Based Brain Tumor Detection and Feature Extraction Using Biologically Inspired BWT and SVM," *Int. J. Biomed. Imaging*, vol. 2017, 2017, <https://doi.org/10.1155/2017/9749108>.
 - [64] Z. Ullah, M. U. Farooq, S. H. Lee, and D. An, "A hybrid image enhancement based brain MRI images classification technique," *Med. Hypotheses*, vol. 143, p. 109922, Oct. 2020, <https://doi.org/10.1016/j.mehy.2020.109922>.
 - [65] M. A. Ansari, R. Mehrotra, and R. Agrawal, "Detection and classification of brain tumor in MRI images using wavelet transform and support vector machine," *J. Interdiscip. Math.*, vol. 23, no. 5, pp. 955–966, 2020, <https://doi.org/10.1080/09720502.2020.1723921>.
 - [66] S. Preethi and P. Aishwarya, "Combining wavelet texture features and deep neural network for tumor detection and segmentation over MRI," *J. Intell. Syst.*, vol. 28, no. 4, pp. 571–588, 2021, <https://doi.org/10.1515/jisys-2017-0090>.
 - [67] U. Raghavendra, A. Gudigar, T. N. Rao, V. Rajinikanth, E. J. Ciaccio, C. H. Yeong, S. C. Satapathy, F. Molinari, and U. R. Acharya, "Feature-versus deep learning-based approaches for the automated detection of brain tumor with magnetic resonance images: A comparative study," *Int. J. Imaging Syst. Technol.*, vol. 32, no. 2, pp. 501–516, Mar. 2022, <https://doi.org/10.1002/ima.22646>.
 - [68] F. lahmood HAMEED and O. DAKKAK, "Brain Tumor Detection and Classification Using Convolutional Neural Network (CNN)," in *2022 International Congress on Human-Computer Interaction, Optimization and Robotic Applications (HORA)*, Jun. 2022, no. 2, pp. 1–7. <https://doi.org/10.1109/HORA55278.2022.9800032>.
 - [69] M. Gupta, S. K. Sharma, and G. C. Sampada, "Classification of Brain Tumor Images Using CNN," *Comput. Intell. Neurosci.*, vol. 2023, pp. 1–6, Oct. 2023, <https://doi.org/10.1155/2023/2002855>.